Dynamic Stress Analysis of Viscoelastic Rotors

A Thesis Submitted to

National Institute of Technology, Rourkela

In partial fulfilment of the requirement for the degree of

Master of Technology

in

Mechanical Engineering

(Specialization-Machine Design and Analysis)

By

Samarth Mishra

(Roll No. 213ME1380)

Department of Mechanical Engineering

National Institute of Technology

Rourkela-769008 (India)

May-2015

Dynamic Stress Analysis of Viscoelastic Rotors

A Thesis Submitted to

National Institute of Technology, Rourkela

In Partial fulfilment of the requirement for the degree of

Master of Technology

in

Mechanical Engineering

(Specialization-Machine Design and Analysis)

By

Samarth Mishra

(Roll No. 213ME1380)

Under the guidance of

Dr. H. Roy

Assistant Professor

Department of Mechanical Engineering, NIT Rourkela

Department of Mechanical Engineering

National Institute of Technology

Rourkela-769008 (India)

May-2015

National Institute of Technology

Rourkela-769008 (Orissa), INDIA

CERTIFICATE

This is to certify that the thesis entitled "**Dynamic stress analysis of viscoelastic rotors**" submitted to the National Institute of Technology, Rourkela by Samarth Mishra Roll No. 213ME1380 for the award of the Master of Technology in Mechanical Engineering with specialization in Machine Design and Analysis is a record of bonafide research work carried out by him under my supervision and guidance. The results presented in this thesis has not been, to the best of my knowledge, submitted to any other University or Institute for the award of any degree or diploma.

The thesis, in my opinion, has reached the standards fulfilling the requirement for the award of Master of Technology in accordance with regulations of the Institute.

Date: 31/5/15

Place: Rourkela

Dr. H. Roy

Assistant Professor

Department of Mechanical Engineering

NIT Rourkela

ACKNOWLEDGEMENT

I would like to thank a true role model, Dr. Haraprasad Roy, who always steered an even keel and never failed to give me his utmost sincere support during the pursuit of this project. Dr. H. Roy's professional dedication is certainly inspiring to anyone who works under him.

I thank specially Saurabh Chandraker and Saurabh Sharma for driving this project towards successful completion.

As for Alok Jha, Bhaskar Vishwakarma, thanks for their immense support, for their guidance and cooperation. I also thank Gaurav, Mrityunjay, Nihar, Ashish and Ajay who brought added meaning and depth to each of my days in NIT Rourkela.

Samarth Mishra

ABSTRACT

The present work deals with the study of stresses in viscoelastic rotor which are dynamic in nature. Due to internal damping of the rotor material, dynamic characteristics get affected and hence it is studied to understand the behavior in terms of Campbell plot, mode shapes etc. This study starts with modelling of beam, where viscoelastic material was considered. The solution for time domain was obtained through state space approach. For discretizing the continuum finite element method is used based on Euler Bernoulli beam theory. Then stresses were found for cantilever beam.

This modelling was further used to model viscoelastic rotor. Stable limit speed as a function for different torque is plotted, which is found to remain constant for varying torques. The bending as well as shear stresses were calculated. For designing of rotor here non-ferrous material was considered as they do not exhibit endurance limit. Then the rotor was analyzed based on dynamic shear and dynamic bending stress, equivalent stresses were obtained and the location which was subjected to maximum stresses was focused and using design equations, life of rotor before failure was found.

NOMENCLATURE

l_e	**Length of an Element**
m_d	**Disc Mass**
D_R	**Diameter of Rotor Shaft/Inner Diameter of a Disc**
D_D	**Outer Diameter of a Disc**
t_D	**Thickness of Disc**
t	**Time in Seconds**
$\bar{y}$	**Half of Depth of Cross-Section of Rotor Shaft/Beam**
q	**Displacement Vector**
$\dot{q}$	**Velocity Vector**
I_r	**Moment of Inertia of Rotor shaft**
A_r	**Area of Cross-Section of Shaft**
T_R	**Magnitude of Applied Axial Torque**
α	**Co-efficient of Thermal Expansion**
ΔT	**Temperature Difference**
P_A	**Axial Thermal Load**
ϕ, θ	**Angles of Rotation about Y and Z Axes**

R_o	**Position Vector of Displaced Centre of Rotation**
E	**Young's Modulus of Elasticity**
ε	**Linear Strain**
M_Y, M_Z	**Bending Moment about Y and Z Axes**
Ω	**Spin Speed**
ω	**Whirl Speed**
L	**Length of rotor shaft**
V_x	**Shear Force**
M_x	**Bending Moment**
μ	**Element Mass Per Unit Length**
ρ	**Volume Density**
η_v	**Viscous Damping Coefficient**
$\{Q\}$	**External Force Vector**
$[M_T]$	**Translatory Mass Matrix**
$[M_R]$	**Rotary Mass Matrix**
$[M]=[M_T]+[M_R]$	**Total Mass Matrix of an Element**
$[G],[K]$	**Gyroscopic and Stiffness Matrices**
$[K_B]$	**Bending Stiffness Matrix**
$[K_C]$	**Skew Symmetric Circulatory Matrix**
$[K_T]$	**Axial Torque Matrix**
$[K_A]$	**Axial Stiffness Matrix**

$\left[\Phi_{xy}\right]$	**Hermite Shape Function in x-y Plane**
$\left[\Phi_{xz}\right]$	**Hermite Shape Function in x-z Plane**
$\left[\Phi\right]$	**Shape Function Matrix**
σ_u	**Ultimate Strength**
$\tilde{\sigma}_{fb}$	**true fracture strength**

Contents

LIST OF FIGURES AND TABLES

CHAPTER 1

Introduction

1.1 Background and Importance

In this era of industrialization, where every work is mechanized. Hence human activities being dependent on machinery, for example long distance travels is done via aero-planes, energy generations done in power plants, and there is computers for all the difficult tasks. All the aforementioned fields use complex mechanisms which include rotating part as an integral part. The demand of present day is efficiency. Hence care is taken to ensure that all different parts integral to the system work with harmony. There is need for the machines being efficient. One of those areas include rotor dynamics considering the rotary parts, since rotating machinery influence vibrations ,which is studied extensively in dynamics.

Rotor dynamics a sub branch of applied mechanics; specializes in dynamics of rotating machinery and structures. It is concerned with behavior and deals with diagnostics of machines under rotatory influence from large systems such as turbo rotors or fans in power plants, those in airplanes(for example-turbojets, helicopter rotors) etc.to the systems which are very small, such as tools used in dentistry, fans of computer ,trimmers etc. The rotor when operating has both rotational energy and energy due to vibration; though in small amounts. The purpose of analysis is to ensure the latter remains to lowest possible limits while in operation. By studying the vibration response one can easily identify problems which may persist even before the actual operation and can prevent failure point of the rotor component which may get precipitated leading to total stall of the machinery.

While designing the rotor of the machine; the necessity to consider their dynamic characteristics leads to further study of rotor dynamics. It is very important during designing of the machine that while functioning at its operating conditions the vibration properties of the rotating machinery remains at the

acceptable region and below the safe limits and during its life (for which it has to be designed) should perform satisfactorily. An unacceptable vibration may lead to the failure of structure. For example as the rotors are supported on the bearings so high values of vibration may lead to breaking of the seals, or it may cause the blades to make contact with the stator part , which is stationary; leading to the large losses as is case in the steam turbines .

We can notice that rotor dynamics may be considered as a sub set of general structural dynamics, but due to rotational motion one can observe the difference from the latter, to account for, the fixed structures do not have inherent forcing, but rotating machines do. Gyroscopic moments induced causes the natural frequency to be a function of rotational speed and varies with same. Centrifugal forces are also introduced causing the stiffening of blade to increase with the rotation speed. Material inherent damping is one another reason.

It has 3 principal components shaft/shaft and disc, bearings and supporting structures and each have their own properties which in turn influences the dynamic behavior of the system. Major component being a shaft (also commonly known as Rotor) with one or more discs and one or more bearings. A rotor is a long slender structure being one dimensional. According to the ISO definition "The rotor is a body suspended through a set of cylindrical hinges or bearings that allows it to rotate freely about an axis fixed in space". The above definition is quite redundant as there are sometimes no bearings (material) to constrain the rotor's rotating axis in the space. There are basically two types of rotors, namely free rotors and fixed rotors. In free rotors there is no constraint and the spin speed is considered constant. And in the case of fixed rotors the speed is accounted by angular momentum.

The analysis of vibration occurring in the machinery is very important in rotating machinery. The vibrations induced, are in majority, caused due to the imbalance forces, which are synchronous to the rotation speed or spin speed. Hence the study of forced vibration becomes crucial in design and analysis

of the rotors. The most commonly used method being the finite element method of analysis. The presence of gyroscopic motions which intern are dependent on the spin speed causes the finite element method to be very complicated and requires large computational steps. But the presence of computers reduces this work to much simpler levels. In finite element method the continua is discretized. The system is divided into smaller regions known as 'elements', which are described by mathematically, which in case of rotor dynamics are differential equations.

1.2 Viscoelasticity

As we know it is property consisting of both viscous and elastic nature. A lot of materials of engineering applications exhibit this property. The difference between simple elastic and viscoelastic behavior is that the elastic materials regain their original state as soon as the force is removed. But in case of viscoelastic materials they may or may not regain its original position as soon as the force is removed. But after certain time it will definitely come to its original position. Hence in case of viscoelastic materials the strain is time dependent for small strains and strain rate comes to play.

1.3 History Of Rotordynamics

By the middle of 19th century a lot work had been done on strings, membranes, plates and beams [25]. But when it comes to the rotation characteristics of these, the success can be attributed to W J Rankine, who in the year 1869 published a paper in which he had propounded that there exists a speed, which he termed as critical speed, for centrifugal whirling. Also Rankine was the first researcher to coin the term 'whirling' [25]. Then D'laval started researching on the subject, since Rankine had not clearly mentioned whether it was possible to reach supercritical speed. D'laval successfully concluded by achieving a rotating machine with steam as the motive force. Laval also gave a relation for whirl radius as a function of shaft eccentricity stiffness and weight. Jeffcott in 1919 published a famous research paper in which he had dealt with supercritical running of the rotor.

His model of rotor was very simple comprising of a massless shaft with a point mass attached to it, commonly known as 'Jeffcott rotor'. Although the model was oversimplified when compared to reality, but it contained quantitative aspects of the rotor exhibiting dynamic behavior. But it fails when complex machines as those in steam and gas turbines, are considered. Since then immense research has been done and more and more complex model have been developed A lot can be said in history but it is very vast, world war and the need for faster jet engines also catalyzed the research in this field. The development of rotor dynamics in early 20^{th} century was motivated by intense evolution of aviation industries.

1.4 Literature survey

Nelson & McVaugh [1] introduced a procedure for modeling a rotor bearing system with rigid discs, discreet bearing and distributed finite rotor elements. Formulation was done in both fixed and rotating coordinates. In their finite element model they considered axial loading, rotary inertia and gyroscopic moments.

Zorzi & Nelson [2] have incorporated both internal viscous and hysteretic damping to provide detailed evaluation of damping rotor stability via FEM both type of damping has been found to produce circulatory terms in general equation of motion, which increases destabilization of the system. Both damping causes nonsynchronous forward precession. The stability effects of anisotropic bearing stiffness & external damping is also demonstrated. As all real materials have the capability of dissipation of mechanical energy, for high speed operation, techniques are required to evaluate the effect of this de-stability mechanism. Linear forms of material damping are used in the finite element scheme which has its own limitation which are overridden when benefits of a stability evaluation are also considered. Finite element simulation of rotor system can be improved by modeling internal friction effects. Viscous damping doesn't increases in stability until first critical speed is reached. Viscous damping provided by bearing characteristics can increases the instability speed threshold.

Cole [5] Examined rotor design optimizations, where vibration response and stability were the main basis of research. Axial distribution of unbalanced components with bounded magnitude was considered for measure of vibration response. Formulation includes gyroscopic effects and bearing coefficients which are time varying in nature. LMI formulation is found to provide flexibility to design for amplitude of vibrations, critical speed and damping level.

Dutt and Nakra [16] rotor speed of a rotor shaft system was analyzed and an approach for determining stability limit was provided. Also the effect of support parameters on stability limit of rotor shaft is studied. The study revealed that by using the viscoelastic supports the stable speed zone could be further increased in hydrodynamic journal bearing.

Muszynska [9] this paper comprises of analytical & experimental study of vertical, overhanging imbalanced rotor by flexible bearing.

Taplak.H [13]. determined the general complex nature of rotors with analytical modeling to investigate the dynamic behavior problems. For this purpose, finite element method is used to analyze the system. For analysis of Campbell diagrams and deformations caused by critical speeds is essential in case of dynamic behavior of rotor. In their study, a program named Dynrot was used to make dynamic analysis. Different mechanical and geometrical properties analysis has been done with Dynrot program for gas turbine rotor system.

Jalali [14] and his researcher concluded failure of the system at high speed due to vibration, the effect of resonant at operating speeds can be reduce by investigation of modal analysis and rectification. Detailed analysis is essential for rotating structure for understanding the dynamic nature of the system. Their work is focused on 3D finite element model, one-dimensional beam-type model and experimental modal test. The Campbell diagram, critical speeds, operational deflection shapes, and

unbalance response of the rotor are obtained in order to completely investigate the dynamic behavior of the rotating system.

Mahesh [5] studied the crankshaft for estimation of life through FEM and for this purpose it was necessary to calculate dynamic load, stresses in the system. Finite element analysis is performed on forged steel crankshaft of four stroke engines to obtain the variation of stress magnitude at critical locations. The dynamic force analysis is carried out analytically using MATLAB program, FE model in ANSYS, and boundary conditions are applied according to the engine mounting conditions. The analysis is carried out for different engine speeds and at different ratio of fillet radius to diameter of crank pin. As a result, critical location on the crankshaft is obtained. The analysis is done to calculate fatigue life using stress-cycle(S-N) approach of crankshaft under complex loading conditions. Due to the repeated bending and twisting, which results in fatigue as the cracks form in the fillet area. An analytical elastic–plastic stress analysis is carried out on metal-matrix composite simply supported beams with transverse uniformly distributed load; of arbitrary orientation.

Gujar-Bhaskar [3] studied dynamometer shaft of inertia dynamometer; which is stepped for predicting fatigue life. Both analytical and finite element method approach were used for the study. This study for predicting fatigue life of inertia dynamometer shaft, under constant amplitude loading provides an insight towards the dynamic behavior of the shaft. Modified Goodman approach was used to estimate the fatigue life. The results obtained from analytical method and finite element methods were in congruence with deviation of about 9%. The stresses were calculated by Von misses criterion. Also system force and acting torque were calculated. Since the shaft considered was a stepped shaft i.e. Varying cross-section lead to the stress concentrations near keyway, around sharp corners. Factor of safety and theoretical number of cycles sustained by shaft before failure was estimated.

Goksenli and Eryurek [4]; their research work was dedicated towards study of drive shaft of a commercial elevator. By visual investigation failure was found to have occurred at the keyways and a typical tensional- bending fatigue fracture surface was detected. Chemical and microstructural properties of the shaft were determined. Stress analysis was performed to find maximum normal and shear stresses at fracture surface. Then fatigue life analysis was performed. This investigation successfully concluded that factor of safety was low, may be due to faulty design or manufacturing of keyway which resulted in radius of curvature being very low and high notch effect. Finite element method was also used to generate results and compared with calculated values.

Hai Jun and Jian [7] Studied a prototype of centrifugal rotor which failed below the designed limit of two times the maximum operation speed in over speed spin testing this paper aimed to find the suitable reason leading to failure analysis and then so provide proper structural enhancement for failure analysis chemical and microstructure analysis was done then in mechanical analysis FE model of 1/24 rotor modes centrifugal load was taken. FEA was also done the analysis indicated that local stress occurred in the hub & edge of tube cavities. By increasing fillet radius peak stress was successfully reduced below the allowable material strength.

Savicki and bravo [26] analytically studied the dynamics & stability of subjected to rubbing due to contact with scab. Thermal effects arising due to the rubbing were accounted for. At various rotating speed, the thermomechanical behavior of the rotor is obtained by numerical simulations. Eight analysis for analysis for stability of rotors with multibearing was also done.

Dowling Norman E [24]: Aim to study mean stress effects for stress life curves & strain life curves. A mathematically consistent method for incorporating the walker approach is developed. Compares Goodman & Morrow equations and the effect of mean stress on stress life and strain life behavior with test data for engineering materials. Goodman equation was found to be excessively conservative.

1.5 Outline of the present thesis

Chapter 1: This chapter introduces the context of the present work. An introduction for recent trends is provided here and then a brief about the history of the rotating machines. Finally literature survey is given.

Chapter 2: Modelling and analysis of beam is considered in the chapter. It starts with the finite element modelling of Euler Bernoulli beam and then stress analysis is also done with Matlab.

Chapter 3: The beam analysis which is done in chapter 2 is taken a step further to be applied to the rotor system. Finite element modelling was done and then a Matlab code was generated. In this chapter.

Chapter 4: This chapter concludes the current work and also provide some suggestions which can take the analysis to further levels.

CHAPTER 2

DYNAMICS OF BEAMS

This chapter is dedicated towards the analysis of simple beams. Equations of motion for euler-bernouli beam is derived. An undamped beam is initially taken and the finite element method was used to discretize the continua and then response in time domain was obtained via state space formulation. Using this the normal stress and strain was calculated for undamped beam. The modelling was further extended considering the damping of the beam. Damping is modelled by Augmenting Thermodynamic field (ATF). Like that of the undamped beam; the study for stress obtained is further extended to those of damped beams. Mode shape and stress curves was plotted for the beam.

2.1 Introduction

A beam is a structure in which transverse forces act. Depending on the end conditions the beam can be simply supported, cantilever etc. In beams one of the dimensions is significantly larger than the other two. The largest is taken as the length and along that direction axis is taken. The cross section perpendicular to the axis may remain constant or may vary with length as is the case of beams with varying cross-section. In engineering practices the beams of 'I','T' type cross-section are commonly found. Wings of aircrafts, lever arms and rims of wheels are type of beams found in mechanical structures, 'I' beams are used in rails.

'Beam theory ' as commonly referred in the solid mechanics theory for beams plays a very crucial role in helping an structural engineer to design satisfactorily according to the design requirements of the structure. As per the mathematical model of the same, it acts as a tool to analyze the structure for various conditions. There more complex modelling the better are the results obtained. Although these since last two decades sophisticated methods like finite element method have been developed which allows us to analyze the structure with much more complexity and the results obtained during the

stages of design can itself allow us to predict the prominent failure conditions, points where stresses obtained are very high. To say in less words these modelling may have ability to give insight to the behavior in pre-design stages. For validating the results (obtained during simulations) it can is quite helpful.

Beam theories based on various assumptions have been developed which arrive at results with different levels of accuracy. One of these was given by Euler Bernoulli which is simplest in nature.it assumes the sections which were plane before bending remains plane after bending i.e. the cross-section is infinitely rigid in the perpendicular plane and hence deformations are absent in the cross section plane. As in Craig and Bauchau [10] the displacement is given as the combination of one translation and one rotation. As the model proposed by Euler Bernoulli does not take into consideration the shear deformation and rotational inertia effect. This approximation hold within good proximity only for long slender beams but not accurate if the beam is thick.

The EB beam was modified by Rayleigh by including the rotational inertia in his model of the beam. The most accurate beam model as developed by Stephen Timoshenko in the onset of 20^{th} century considers both rotational inertia and shear deformation, which was considered accurate for describing short, thick beams. Due to addition of shear deformation term, the assumption of cross section remaining perpendicular to the centerline before and after bending is relaxed and can suitably be accounted for.

2.2 Equation of motion of undamped Euler Bernoulli beam

The schematic diagram of the beam element considered is shown in the below figure which is subjected to bending moments and shear force. Also an external force F(x, t) also acts.

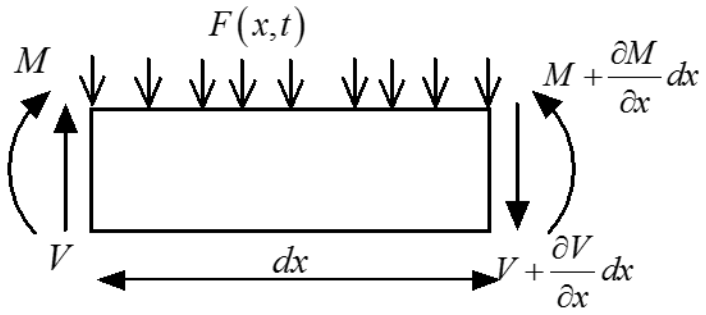

FIGURE 2.1: A SECTION OF EULER-BERNOULLI BEAM

Apply equilibrium of force in Y-direction for the above beam section i.e. $\sum F_x = 0$

$$\left(V + \frac{\partial V}{\partial x}dx\right) - V + Fdx = \rho A \frac{\partial^2 y}{\partial t^2}dx \qquad 2.1$$

The above equation is simplified as :

$$\frac{\partial^2 y}{\partial t^2} + \frac{\mathrm{EI}}{\rho A}\frac{\partial^4 y}{\partial x^4} = 0 \qquad 2.2$$

Similarly the momentum equilibrium is also applied

$$\sum M_x = 0$$

$$\left(M + \frac{\partial M}{\partial x}dx\right) - M - Vdx + F\frac{dx}{2}dx = 0$$

$$\left(\frac{\partial M}{\partial x}dx\right) - Vdx + F\frac{dx}{2}dx = 0 \qquad 2.3$$

simplyfiing the above equation and neglecting the term $dx/2$ *we get* the equation as follows :

$$V = \frac{\partial M}{\partial x} \qquad 2.4$$

The bending moment is written according to beam theory as:

$$M = -EI\frac{\partial^2 y}{\partial x^2} \qquad 2.5$$

Then we get V (shear force) as

$$V = -EI\frac{\partial^3 y}{\partial x^3} \qquad 2.6$$

Differentiating the above equation w.r.t. x

$$\frac{dV}{dx} = -EI\frac{\partial^4 y}{\partial x^4} \qquad 2.7$$

using equation 2.7 in the equation 2.2

$$-EI\frac{\partial^4 y}{\partial x^4} - \rho A\frac{\partial^2 y}{\partial t^2} = -F$$

rearranging the above equation we get

$$EI\frac{\partial^4 y}{\partial x^4} + \rho A\frac{\partial^2 y}{\partial t^2} = F \qquad 2.8$$

rearranging the above equation we get

$$\frac{\partial^2 y}{\partial t^2} + \frac{EI}{\rho A}\frac{\partial^4 y}{\partial x^4} = 0$$ .....is the required governing equation for Euler Bernoulli Beam

2.3 Elastic Beam Finite Element Formulation

The Galerkin residual method is employed in the preceding equation to obtain the finite element form

$$\int_0^{l_e} \left[\phi_{xy}\right]^T \left(EIy'''' + \rho A\ddot{y}\right) dx = 0 \qquad 2.9$$

Where EI is constant and $(\phi_{xy})_i$ are the usual cubic shape functions, the integration by parts of the fourth derivative term in the equation 2.9 yields

$$\int_0^{l_e} \left[\phi_{xy}\right]^T y'''' dx = \int_0^{l_e} \left[\phi_{xy}\right]^T y'' dx + \left[\left[\phi_{xy}\right]^T y''' - \left[\phi'_{xy}\right]^T y''\right]_0^{l_e} \qquad 2.10$$

$$\int_0^{l_e} \left(\left[\phi''_{xy}\right]^T EIy'' + \rho A\left[\phi_{xy}\right]^T \ddot{y}\right) dx = 0 = \left[\left[\phi_{xy}\right]^T V - \left[\phi_{xy}\right]^T M\right]_0^{l_e} \qquad 2.11$$

terms V and M will be part of the load vector $\{F\}$

$$\ddot{y} = \left[\phi_{xy}\right]\{\ddot{q}\} \text{ and } y'' = \left[\phi''_{xy}\right]\{q\} \qquad \left[\phi''_{xy}\right] = [B]$$

$$\{q\} = \left[\nu_1 \;\; \psi_1 \;\; \nu_2 \;\; \psi_2\right] \text{ and } y'' = \left[\phi''_{xy}\right]\{q\}$$

where $[m]$ and $[k]$ are global mass matrix and global stiffness matrix

$$[k]\{q\}_j + [m]\{\ddot{q}\}_j = \{F\} \qquad 2.12$$

When the size of above matrices are expanded as according to that of the structure size then equation 2.12 will be the standard equation of motion;

where $[m]$ and $[k]$ are global mass matrix and global stiffness matrix

$\sigma = E\varepsilon - \delta\xi$; $H = \delta\varepsilon - \gamma\xi$ [8]

$\bar{\xi}$ is the value of ξ at equilibrium and is obtained as

$$\delta\varepsilon - \gamma\bar{\xi} = 0 \qquad 2.13$$

$$\bar{\xi} = \frac{\delta\varepsilon}{\gamma} \qquad 2.14$$

$$\dot{\xi} = -b\left(\xi - \bar{\xi}\right) \qquad 2.15$$

Using eqn. 2.14 in eqn. 2.15 we get

$$\dot{\xi} + b\xi = \frac{b\delta}{\gamma}\varepsilon \qquad 2.16$$

$$\left(D + b\right)\xi = \frac{b\delta}{\gamma}\varepsilon \qquad 2.17$$

$$\xi = \frac{b\delta}{\gamma(D+b)}\varepsilon$$

Using above equation in equation 2.13 and neglecting the term $\frac{D}{b}$, as b>>0

$$\sigma = (a_0 + a_1 D)\varepsilon \qquad 2.18$$

$$where\ \mathrm{a}_0 = E - \frac{\delta^2}{\gamma}\ \text{and}\ \mathrm{a}_1 = \frac{E}{b}$$

we have equation of motion as:

$$M\ddot{q} + Kq = 0\ \ where\ \mathrm{K} = \frac{EI}{l_e^3}\int_0^{l_e}\left[\phi''_{xy}\right]^T\left[\phi''_{xy}\right]dx \qquad 2.19$$

Solving the equation 2.18 we finally arrive at the structural equation of motion where damping matrix is incorporated by modifying the stiffness matrix as:

$$[C] = \frac{EI}{Bl_e}\int_0^{l_e}\left[\phi''_{xy}\right]^T\left[\phi''_{xy}\right]dx \qquad 2.20a$$

$$[K] = \frac{I}{l^3{}_e}\left(E - \frac{\delta^2}{\gamma}\right)\int_0^{l_e}\left[\phi''_{xy}\right]^T\left[\phi''_{xy}\right]dx \qquad 2.20b$$

Mechanical strain and stress in finite element form is given by

$$\in_x = \bar{y}\left[\phi''_{xy}\right]^T\{q\}, \qquad 2.21a$$

$$\sigma_x = E\bar{y}\left[\phi''_{xy}\right]^T\{q\} \qquad 2.21b$$

2.4 Beam: A Numerical Problem

A cantilever beam having a rectangular cross-section was studied. It was discretized into finite elements. An Euler-Bernoulli beam element was considered as modelled in earlier section. Frequency response and mode shape were plotted for the beam. For this Matlab code is written and Eigen values and Eigen vectors were found. Shown below is the schematic diagram of the cantilever beam with an end load, load being harmonic in nature.

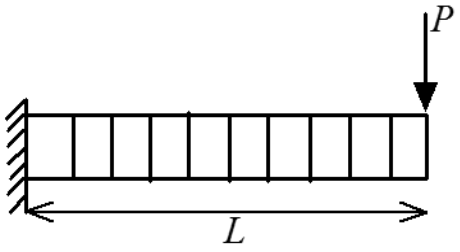

FIGURE 2.2: DISCRETIZED CANTILEVER BEAM

Data for the cantilever beam considered:

Material is aluminum 2024-T3, material density (ρ) =2700 kg/m^3, Young's modulus (E) =7×10^{11} N/mm^2,

Amplitude of applied force=5N, length of the cantilever beam=4m, Width=0.08m, Height=0.2m

In figure 2.3, mode shapes for the 1st three modes are plotted with respect to nodes. Mode shape shows relative displacements of the degrees of freedom i.e. is a motion pattern where system vibrates or moves in phase and with same frequency.

The Frequencies exhibited by normal modes are known as resonance frequency or natural frequency. Figure 2.4 represents a plot between applied frequency and Response amplitude, obtained at the free end of the beam with external sine function applied at the free end of the cantilever beam considered.

The plot is displacement amplitude; obtained for different frequencies, from equation of motion

The response for the free end of the cantilever beam as a time dependent function is obtained. The formulation was done using state space method.

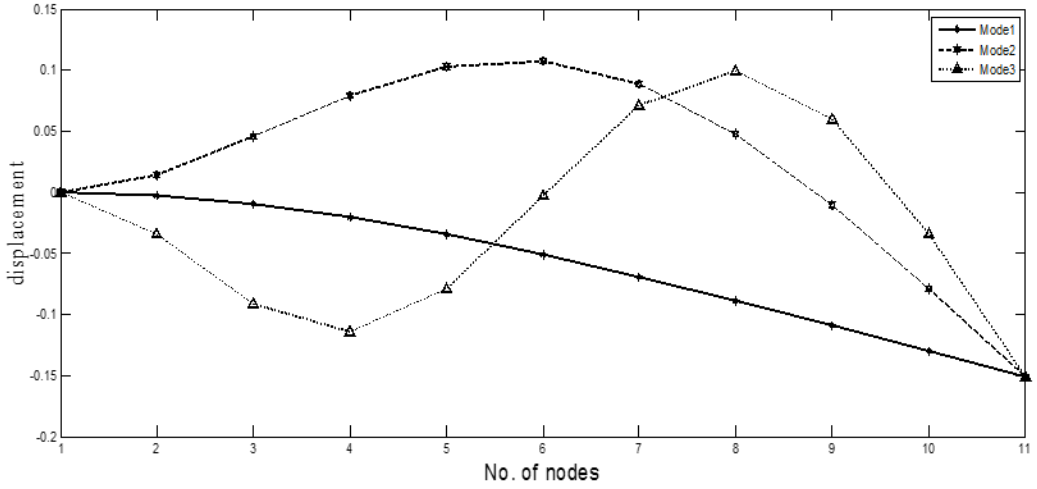

FIGURE 2.3: MODE SHAPES VERSUS NODES

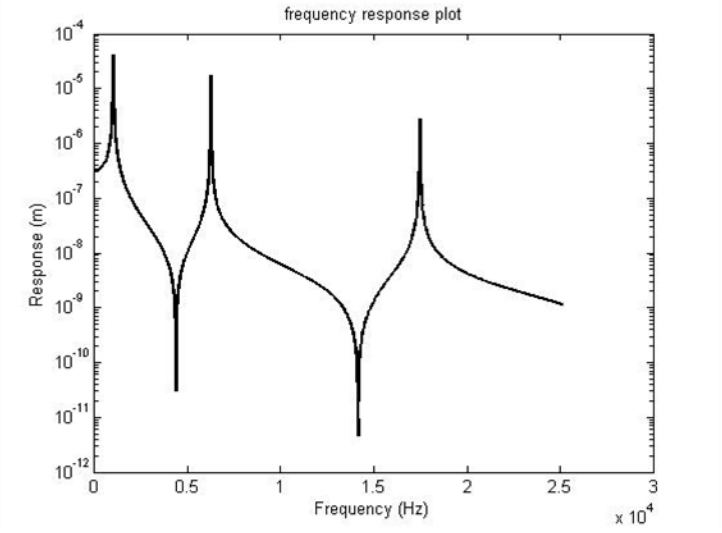

FIGURE 2.4: RESPONSE VERSUS FREQUENCY

Now response of the tip of cantilever beam with time is plotted in the below figures for undamped system. Figure 2.5 depicts amplitude versus time response and figure 2.6 shows variation of stress with time for the undamped beam considered. Response was calculated by forming state-space form. We can see that both the curves exhibit same nature, hence steady state fluctuation is obtained.

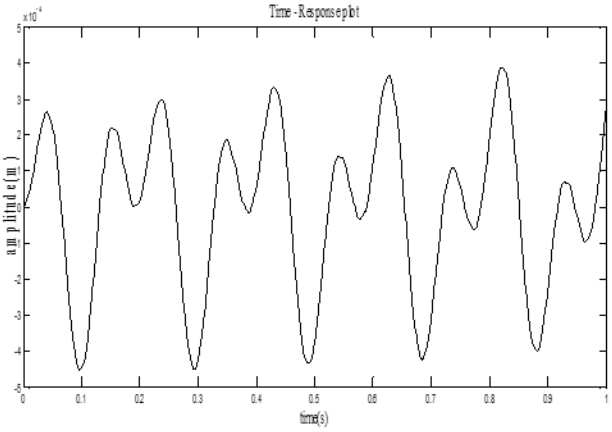

FIGURE2.5: TIME RESPONSE

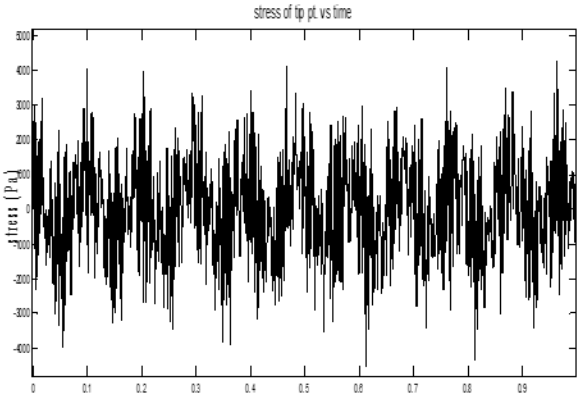

FIGURE2.6: STRESS AT THE TIP OF UNDAMPED BEAM

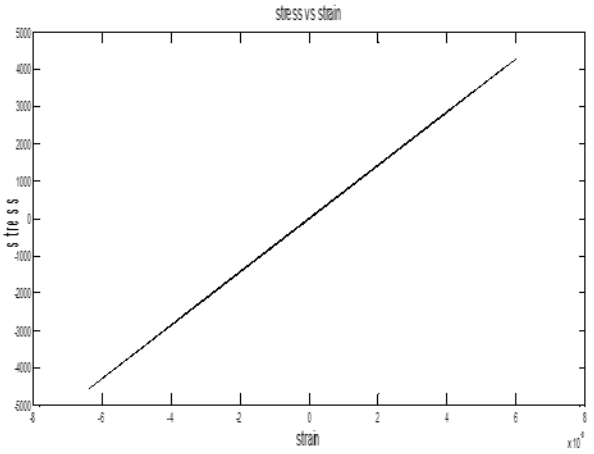

FIGURE2.7: STRESS VERSUS STRAIN FOR UNDAMPED BEAM

In the above figure stress versus strain is plotted for the above considered undamped cantilever beam. It is same as that of the elastic stress-strain condition i.e. a straight line is obtained.

This study is further continued for damped system. Damping is achieved in earlier section as in [8]. Where β, δ and γ are augmented thermodynamic field parameters [8].

The trend can be seen from the response plot and stress plot in the figures 2.8 and 2.9, the amplitude is constant. Hence the system is under steady state excitation.

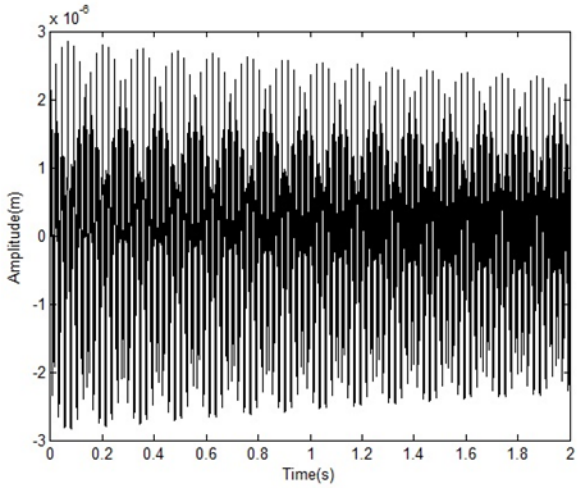

FIGURE2.8 RESPONSE TIME PLOT FOR FREE END OF THE DAMPED BEAM

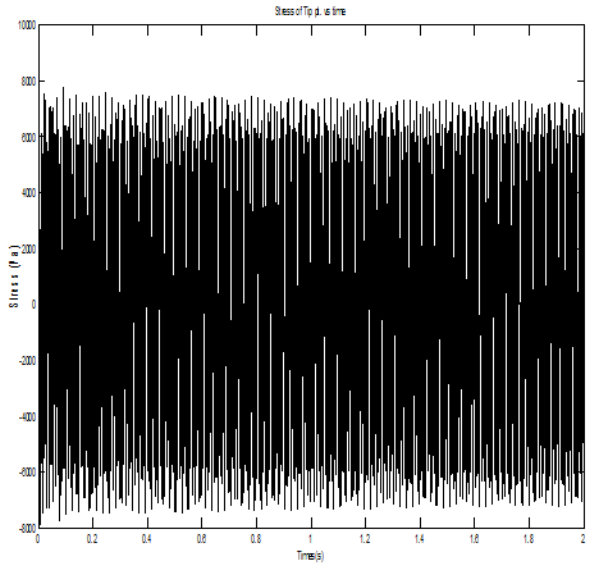

FIGURE2.9 STRESS TIME PLOT FOR FREE END OF THE DAMPED BEAM

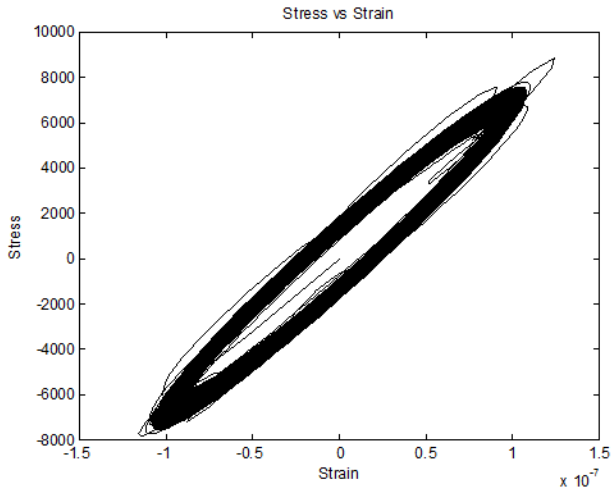

FIGURE2.10: STRESS STRAIN PLOT FOR FREE END OF THE DAMPED BEAM

Figure 2.7 shows the stress strain graph for undamped system is a straight line i.e. follows hook's law, for elastic materials. In case of damped system, as there is energy dissipation, the stress strain plot is found to be elliptical in nature as in figure 2.10

CHAPTER 3

ANALYSIS OF ROTORS

3.1 Dynamics

In the dynamics section mathematical modelling of rotor by finite element method is done. Here dynamic characteristics of simple rotor is considered. Here the system is discretized in a simple way leading to a finite model with finite number of coordinates. The motion considered here is two plane motion and gyroscopic effect is also considered. The finite element code developed was validated with the published results.

3.1.1 Mathematical formulation

Here in the formulation section, rotor shaft viscoelastic in nature is considered. Based on earlier developed Euler Bernoulli beam element, the finite rotor element is two plane bending. The finite element modelling for the before mention rotor is shown. For viscoelastic modelling Kelvin Voigot model was considered. In Kelvin Voigot model stiffness is represented with spring (hookean spring); damping with dashpot (Newtonian damper), both connected in parallel connection as shown in the figure 3.1

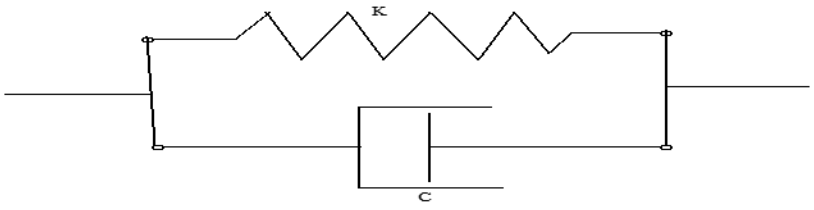

FIGURE 3.1: DIAGRAM OF KELVIN-VOIGOT MODEL

3.1.2 Finite Element Model

The shaft cross-section in displaced position is shown in figure 3.2. According to the figure 3.2 the displacement in Y-direction is indicated as v and the displacement in Z-direction is w. Let Ω is the spin speed (radian/seconds) and ω is the whirl speed. After time t consider a differential element with thickness dr, r is the distance from the center of the shaft, the angle subtended is $d\Omega t$,where Ωt varies from 0 to 2π.As there occurs transverse vibrations two types of rotation occurs , firstly spin of the rotor about its own axis and secondly, whirl motion.

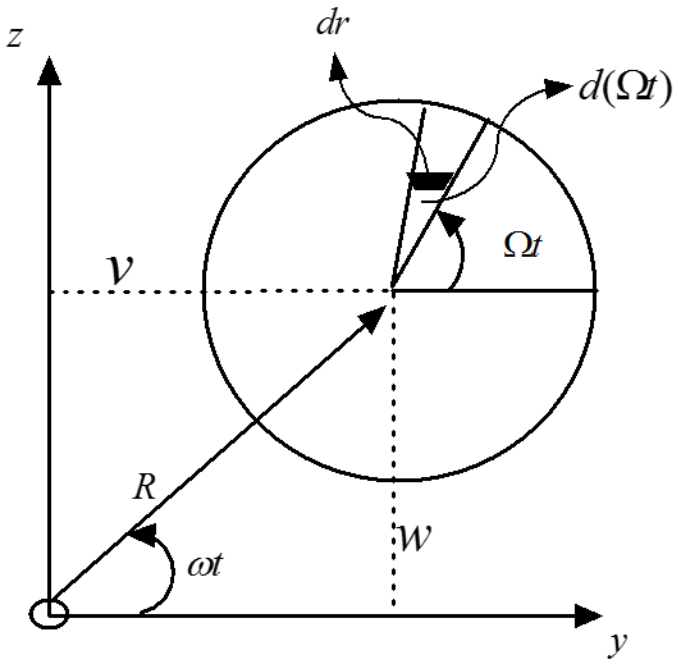

FIGURE: 3.2: SCHEMATIC SHOWING DISPLACED CROSS-SECTION OF THE SHAFT

Longitudinal stress and strain induced in the element of area ($(d\Omega t)rdr$) shown in above figure are σ_x and ε_x. The stress are dynamic in nature. As per reference [2] Zorzi and Nelson, the expression for σ_x and ε_x at a given instant of time is:

$$\sigma_x = E\left(\varepsilon + \eta_v \dot{\varepsilon}\right) \quad \text{and} \quad \varepsilon_x = -r\cos\left[\left(\Omega - \omega\right)t\right]\frac{\partial^2 R(x,t)}{\partial x^2} \tag{3.1}$$

At any instant the bending moment about y and z axis, according to Zorzi and nelson [2] are

$$M_{xx} = \int_0^{2\pi}\int_0^{r_0} -\left(v + r\cos\left(\Omega t\right)\right)\sigma_x \, r dr \, d\left(\Omega t\right) \tag{3.2a}$$

$$M_{yy} = \int_0^{2\pi}\int_0^{r_0} -\left(w + r\cos\left(\Omega t\right)\right)\sigma_x \, r dr \, d\left(\Omega t\right) \tag{3.2b}$$

Using equation 3.2 we get governing equation for a shaft element is a differential equation as given below

$$\left[M_T\right] + \left[M_R\right]\left\{\ddot{q}\right\} + \left(\eta_v\left[K_B\right] + \Omega\left[G\right]\right)\left\{\dot{q}\right\} + \left(\left[K_B\right] + \eta_v\Omega\left[K_c\right] + \left[K_T\right] - \left[K_A\right]\right)\left\{q\right\} = \left\{F\right\} \tag{3.3}$$

Where $\left[K_c\right], \left[K_A\right], \left[K_B\right], \left[K_T\right], \left[M_R\right], \left[M_T\right], \left[G\right]$ are skewsymmetric circulation matrix, axial stiffness matrix, bending stiffness matrix, stiffness matrix due to externally applied torque, matrix for rotary inertia, translational mass matrix, gyroscopic matrix. $\{q\}_{8\times1}$ is nodal displacement vector and η_v is viscous damping coefficient. This equation is the full structural equation of motion for the shaft. $\left[K_T\right]$, $\left[K_A\right]$ were incorporated after referring to Zorzi nelson [2] and Robert cook [16] . Expressions for various matrix used in equation 3.3 are listed below. Further refer to the appendix for elements in the matrices

$$\left[M_R\right] = \int_0^{l_e} \rho A\left[\phi(x)\right]\left[\phi(x)\right]^T dx, \qquad \left[M_T\right] = \int_0^{l_e} \rho I\left[\phi'(x)\right]\left[\phi'(x)\right]^T dx,$$

$$[K_B]=\int_0^{l_e} EI[\phi''(x)][\phi''(x)]^T\,dx \qquad [K_C]=\int_0^{l_e} EI[\phi''(x)]\begin{bmatrix}0 & 1\\ -1 & 0\end{bmatrix}[\phi''(x)]^T\,dx$$

$$[G]=\int_0^{l_e} 2\Omega\rho I[\phi'(x)]^T\begin{bmatrix}0 & 1\\ -1 & 0\end{bmatrix}[\phi'(x)]dx$$

$$[K_T]=\int_0^{l_e} T_A[\phi''(x)]^T\begin{bmatrix}0 & 1\\ -1 & 0\end{bmatrix}[\phi''(x)]dx \qquad \{q\}=\{\mathrm{v}_1\ \psi_1\ \mathrm{w}_1\ \theta_1\ \mathrm{v}_2\ \psi_2\ \mathrm{w}_2\ \theta_2\}^T$$ The matrix for Hermite's shape function $\phi(x)$ is given as:

$$[\phi(x)]=\begin{bmatrix}\{\phi_{xy}(x)\} & \{0\}\\ \{0\} & \{\phi_{zy}(x)\}\end{bmatrix}$$ Where subscripts xy represent XY plane and yz represents YZ plane.

Due to thermal expansion there will be an axial load given by relation $P_A=E\alpha\left(\bar{T}-T_0\right)$, where α is coefficient of thermal expansion, $\bar{T}$ is the average temperature and T_0 is the reference temperature over the cross section. T_A applied axial torque applied externally, A is the crossectional area, ρ is density, E is the young's modulas of the material of the rotor and I is the moment of inertia of the cross section of rotor.

3.2 Fatigue analysis

$$\in_x = \bar{y}\left[\phi''(x)\right]^T \{q\} \quad 3.4$$

$$\dot{\in}_x = \bar{y}\left[\phi''(x)\right]^T \{\dot{q}\} \quad 3.5$$

Where $\bar{y}$ is the distance of neutral axis of the shaft from top fiber.

The bending stress which gets developed in axis direction will be given by the following relation:

$$\sigma = E\left(\in + \left(\eta_v \times \dot{\in}\right)\right) \quad 3.6$$

Now putting values of $\dot{\in}$ and $\in$ in the above equation we get

$$\sigma_x = E\bar{y}\left(\left[\phi''(x)\right]^T \{q\} + \left(\eta_v \times \left[\phi''(x)\right]^T \{\dot{q}\}\right)\right) \quad 3.7$$

From theory of beams, the relation between shear force and bending moment is given as

$$\frac{M}{I} = \frac{\sigma_x}{\bar{y}} \quad \text{and} \quad V = \frac{dM}{dx} \quad 3.8$$

After using equation 3.8 in equation 3.7 we obtain the shear force relation as developed in viscoelastic material as:

$$V_x = E \times I_r \times \left[\left(\left(\Phi'''(x)\right)^T \times \{q\}\right) + \left(\eta_v \times \left(\Phi'''(x)\right)^T \times \left\{\dot{q}\right\}\right)\right] \quad 3.9$$

Maximum shear stress for shaft having circular cross section is given by:

$$\tau_{max} = \left(\frac{4}{3}\tau_{avg}\right) \quad 3.10$$

Since the loading is under dynamic conditions, hence there will be a maximum and minimum normal stress and shear stress developed. Based on which we will find mean and alternating stress.

$$\sigma_a = \frac{\sigma_{max} - \sigma_{min}}{2} ; \sigma_m = \frac{\sigma_{max} + \sigma_{min}}{2} \quad 3.11$$

In equation 3.11 the subscript 'm' stands for the average value of stress and the subscript 'a' stands for variable or alternating value of the stress [20]. Similarly the alternating and mean shear stresses can be calculated from fluctuating shear stresses as

$$\tau_m = \frac{\tau_{max} + \tau_{max}}{2} \text{ and } \tau_a = \frac{\tau_{max} - \tau_{max}}{2} \quad 3.12$$

Using distortion energy theory [22], equivalent dynamic mean and stresses are calculated as:

$$(\sigma_{eq})_m = \sqrt{(\sigma_m)^2 + 3 \times (\tau_m)^2} \text{ and } (\sigma_{eq})_a = \sqrt{(\sigma_a)^2 + 3 \times (\tau_a)^2} \quad 3.13$$

Initially to analyze for fatigue we should have the failure stress, for the combination of obtained equivalent mean and variable stress. In case of ferrous material we use endurance limit as the basis for design but if using non-ferrous materials as earlier discussed in chapter 1, there is no endurance limit and hence we find out equivalent stress that would cause the same life as that by the given combination of the mean equivalent stress and equivalent variable stress. In reference [24] it was suggested that to use various other empirical relations for the calculation of the same. Once we have the equivalent stress, using the Basqin's equation we can calculate the life of the rotor. Two of the empirical relations used in the analysis have been listed below.

GOODMAN EQUATION

$$\frac{\sigma_a}{\sigma_{ar}} + \frac{\sigma_m}{\sigma_u} = 1 \qquad 3.14$$

This is the modified Goodman relationship as formulated by J. O. Smith [24]. It is useful to solve for σ_{ar}, which is defined as completely reversed stress that is expected to cause the same life as the actual combination of amplitude stress and mean stress.

MORROW EQUATION

Morrow [24] suggested modifying the Goodman relationship by employing the true fracture strength as the intercept

$$\sigma_{ar} = \frac{\sigma_a}{1 - \frac{\sigma_m}{\tilde{\sigma}_{fB}}} \qquad 3.15$$

Where $\tilde{\sigma}_{fb}$ is the true fracture strength.

The life of the rotor was calculated using Basqin equation

$$\sigma_{ar} = \sigma'_f (2N_f)^b \qquad 3.16$$

Where N_f is Cycles to failure and the fitting constants (σ'_f) and 'b' are determined from tests under zero mean stress, also called completely reversed tests. Writing the equation in terms of N_f, we get the following relation

$$N_f = 0.5\left(\frac{\sigma_{ar}}{\sigma'_f}\right)^{\frac{1}{b}} \qquad 3.17$$

NUMERICAL PROBLEM

3.3 Finite Element Code Validation

A three disc rotor shaft system is shown in figure 3.4 as in Lalanne and Ferraris [11]. The system considered is simply supported and has three discs of different size. No axial load and axial torque is considered. Hence $P_A = 0$ and $P_T = 0$. Some of the results are shown as tabulated for the purpose of validation.

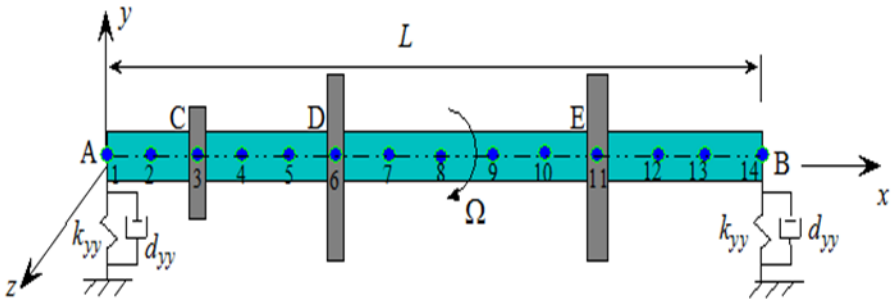

FIGURE 3.3: LALANNE ROTOR: SCHEMATIC DIAGRAM

The material properties of the rotor is shown in table 3.1 as well as table 3.2 which contains material properties of the steel rotor which was used in the paper [11] and dimensions as well as mass unbalance of the discs. The discs were positioned at 3rd, 6th and 11th nodes. The second disc which is at 6th node is unbalanced and it is 200gm-mm.

TABLE 3.1: ROTOR PROPERTIES

Material	Density (kg/m^3)	Young's Modulus (GPa)	Length (m)	Diameter (m)	Coefficient of Viscous Damping (s)
Mild steel	7800	200	1.3	0.2	0

TABLE 3.2: DIMENSIONS OF THREE DISCS AND UNBALANCE

Disc	Diameter (m)	Thickness (m)	Mass unbalance (kg-m)
1	0.24	0.05	0
2	0.40	0.05	2×10^{-4}
3	0.40	0.06	0

Figure 3.4 shows the Campbell plot for the Lalanne rotor considered here. A Campbell diagram [23] is a plot which is plotted between the whirl frequencies as the ordinates and spin speed is plotted as abscissa. It gives whirl lines, which are of two types forward whirl line and backward whirl line. Then there is synchronous whirl line which is a 45^0 line. The point at which synchronous whirl line cuts the forward and backward whirl lines is known as points of critical frequency i.e. the intersection gives critical frequencies.

Then frequency response can be seen in figure 3.5.The peaks which can be seen in the figure of frequency response are the points of resonance occurring in system. As we know that the when frequency of forcing function and natural frequency of system becomes equal then resonance occur. So the point of resonance as obtained in the plot are points of unstability i.e. the system is at the risk of failure. These critical frequencies, which causes large amplitude of vibrations, are to be avoided so that the system is stable and safety is ensured.

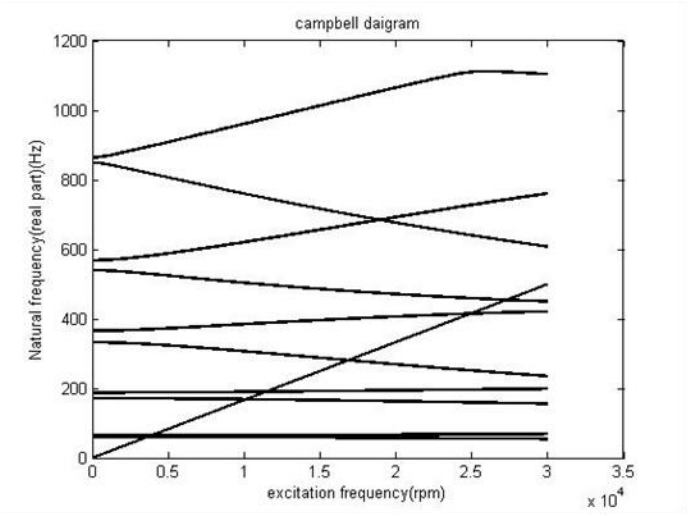

FIGURE3.4 CAMPBELL PLOT

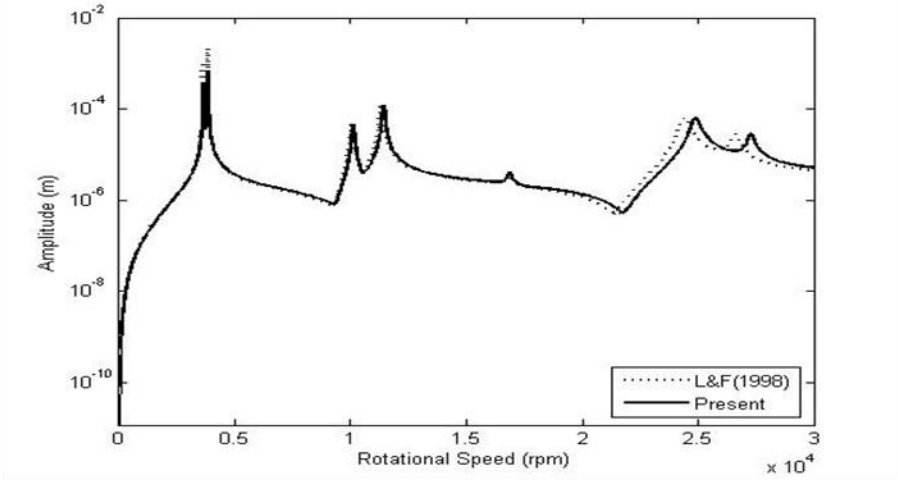

FIGURE 3.5 RESPONSE FOR MASS UNBALANCE

To find the system stability the eigenvectors and eigenvalues were calculated. As can be seen in the table below, the computed values and those of Lalanne and Ferraris [11], match very closely. Thus the formulated code is validated.

TABLE 3.3 VALIDATION OF FREQUENCY

S.No	Frequency	Present result	L&F (1998)
1	F1	54	55.41
2	F2	68	67.20
3	F3	154	156
4	F4	196	193.6
5	F5	232	241.9
6	F6	415	407.5
7	F7	444	446.7
8	F8	596	714
9	F9	750	622.7
10	F10	1085	1077

3.4 Single Disc Rotor

A rotor shaft having aluminum alloy with simply supported bearing at the ends with a disc at the central position is taken into consideration. The rotor is subjected to thermal load, as there is temperature difference with environment. An external torque is applied. Modelling of the bearing is done as a flexible damped supports having damping and stiffness coefficients $\left(c_{yy}, k_{yy}\right)$ and $\left(c_{zz}, k_{zz}\right)$ in xy and zx planes respectively. In figure 3.6 the schematic diagram for the rotor shaft system is shown.

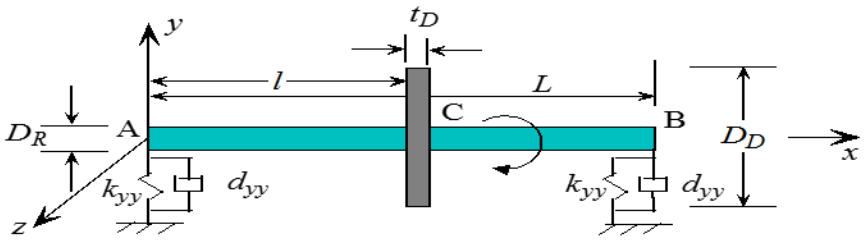

FIGURE 3.6: SCHEMATIC DIAGRAM OF SINGLE DISC ROTOR

Data for the above system is as follows:

$k_{yy} = k_{zz} = 7\times10^{7}$ N/m, $c_{yy} = c_{zz} = 7\times10^{2}$ N/m, length of the shaft is L=1 m, rotor diameter D_R=0.07, disc diameter D_D=0.4m, disc thickness D_T=0.05m. The unbalance in the disc considered is U= 200gm mm. Disc Node= 6^{th}

Material properties are:

Material=2024-T3 Al, Yield stress (σ_o) = 359 MPa, Ultimate stress (σ_u) = 497 MPa, Fracture stress ($\tilde{\sigma}_{fB}$) = 610 MPa, Young's modulus (E) = 73×10^{9} Pa, density (ρ) =2770kg/m^3, η_v =2×10^{-4} seconds.

For the analysis of fatigue a damped rotor shaft with a disc at the central position is considered. The damping here is internal damping. The continuous rotor shaft system is broken into ten elements i.e. discretization is done into ten elements.

Based on the formulation in finite elements, a Matlab code was written to simulate numerically the rotor. The disc considered is at the middle node and unbalance was taken equal to 2×10^{-4} kg-m. Then Eigen vectors and Eigen values were calculated. The Eigen values have two parts-a real part and an imaginary part. When real parts are plotted against spin speed, a decay rate plot is generated. This plot gives us the limit of spin speed for which the system will remain stable. After this spin speed the system will become unstable.

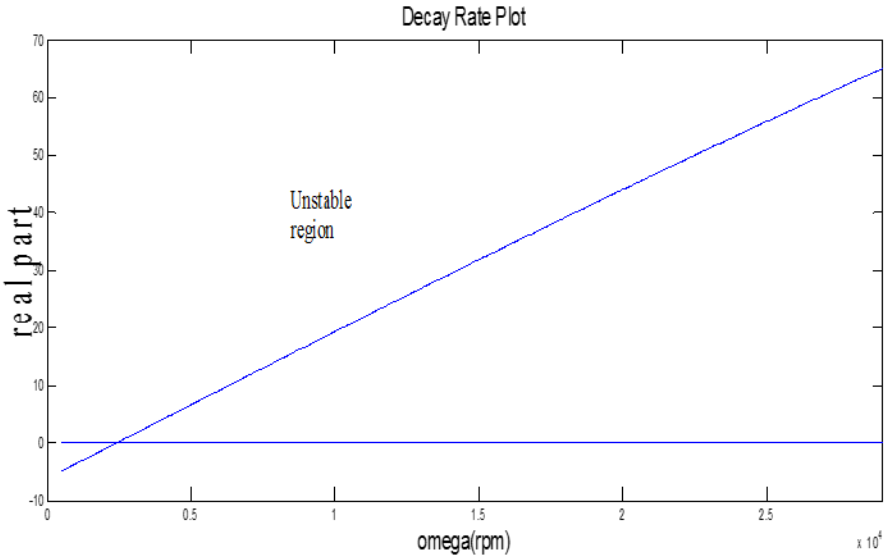

FIGURE3.7: DECAY RATE PLOT

As can be seen from the decay rate plot which can be seen in figure 3.7 the maximum real plot increases from maximum negative to positive as the spin speed increases. The point corresponding to the intersection of the two lines will give us the spin speed which is also known as 'stability limit speed'. It was found to be 2426 rpm.

With this stability limit speed (SLS) as obtained in decay rate plot, a plot of SLS with different torque was plotted, which is shown in the figure 3.8.

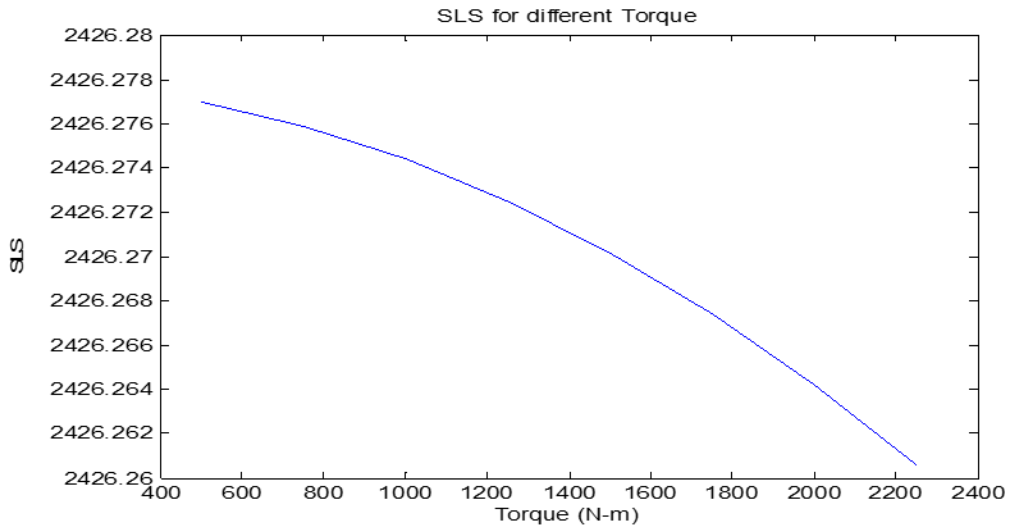

FIGURE3.8**:** SLS VERSUS TORQUE

As can be seen from the above figure of SLS vs torque, the stability limit speed does not vary with the varying torques. Hence stresses are calculated at 2426 rpm and 500 N-m. Based on the calculated stresses i.e. bending stress, shear stress and equivalent stress, plot was generated for different time instances and are shown in figures 3.9-3.11.

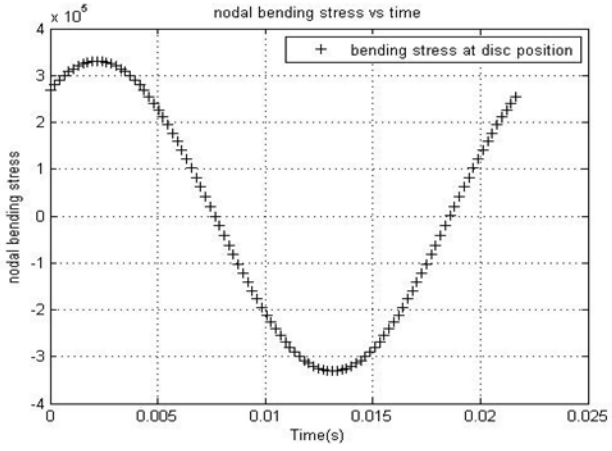

FIGURE 3.9a: BENDING STRESS VERSUS TIME

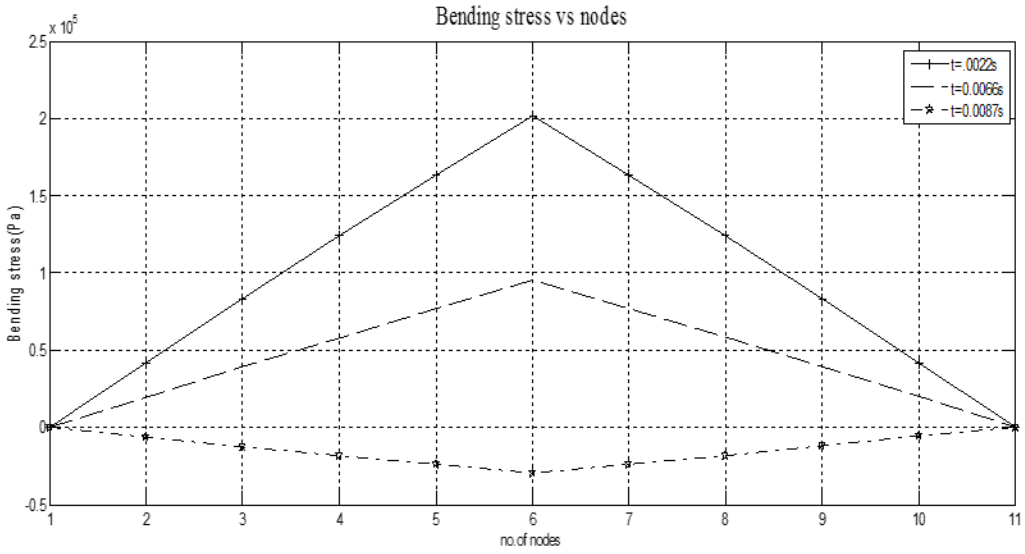

FIGURE 3.9b: BENDING STRESS VERSUS NODES

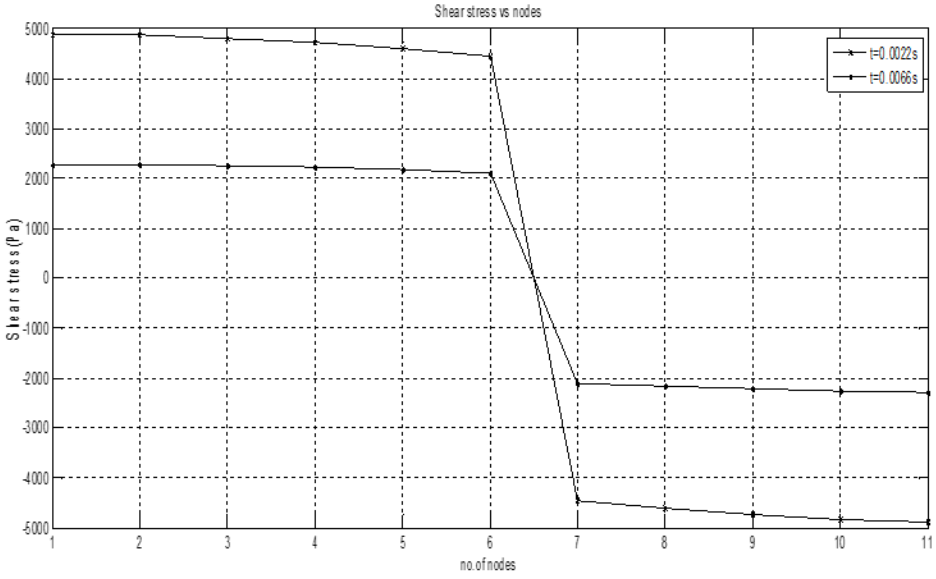

FIGURE 3.10: SHEAR STRESS VERSUS NODES

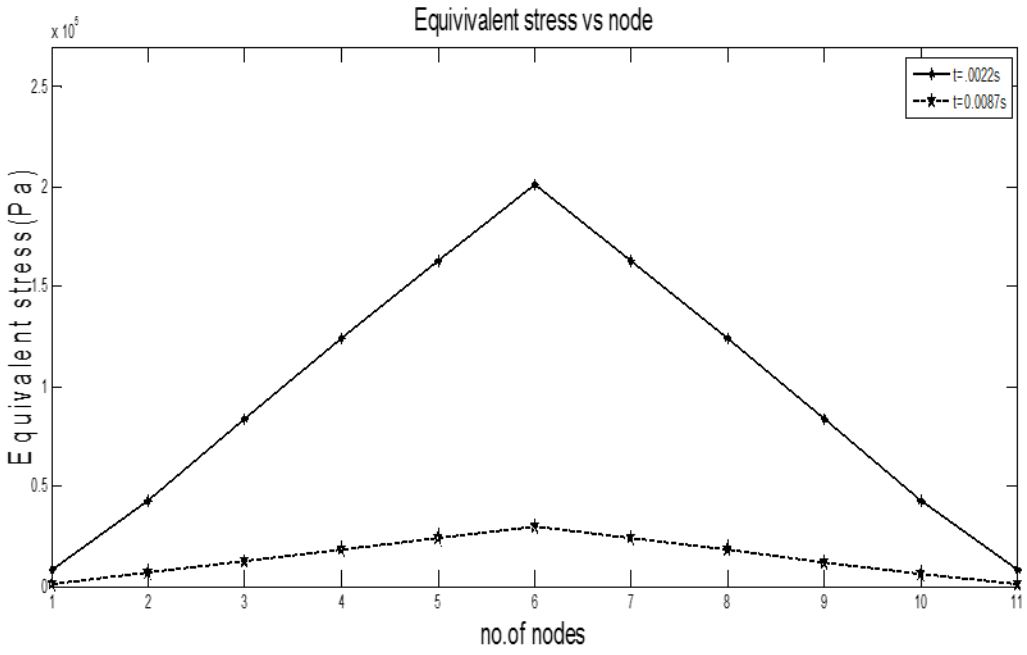

FIGURE 3.11 EQUIVALENT STRESS VERSUS NODES

Referring to figure 3.11, we can easily notice that for different time instant equivalent stress obtained at the 6th node i.e. disc position is very high and it is considered as the design point for later analysis.

Now to design the rotor shaft for fatigue the center of the shaft will be taken as the design point. For this purpose we will calculate σ_{ar}, which is defined as completely reversed stress that is expected to cause the same life as the actual combination of amplitude stress and mean stress. Using two of the empirical relations as that of Goodman relation that modified by J.O Smith and the Morrow equation. This stress is determined on the basis of maximum stress occurring at mid-point.

Then the life of the rotor based on the stress calculated above is obtained by Basqin's equation. Life of the rotor is defined as the number of cycles to failure. The life obtained as from simulation is listed in the following table

TABLE 3.4: LIFE OF THE ROTOR

Empirical equation used	Life of the rotor obtained
Modified Goodman	1.8735×10^7
Morrow	1.8964×10^7

CHAPTER 4

4.1 Conclusion

Based on the literature survey done it was felt that there was a need to study the stresses generated and aim was to study for failure in fatigue. As per shaft line theory which considers the modelling of rotors with two plane bending elements for study of rotor dynamics. Hence first the finite element modelling of a beam based on Euler-Bernoulli beam was done. Rotary inertia was also included in the modelling. The damping was achieved by considering viscoelastic damping. A numerical example was taken to understand the modelling and analyze the correctness. The stress analysis was also done and the results were plotted for both undamped and damped case of the beam. The results were found to be in agreement with other published results.

Then for rotor modelling the finite element of the beam was taken a step further to two plane bending and analysis was done. A Matlab code is generated and validated for unbalance response and frequency responses. The results were very near to the published results of Lalanne and Ferraris [11] thus validating the code. For fatigue analysis numerical problem a non-ferrous material was taken into consideration and single disc shaft system is taken. From the plot of equivalent stresses versus nodes it was asserted that there was maximum stress at the central position. Hence the disc position which was central position was taken as the design point for failure. Then the life of the rotor was found to be 1.8×10^{7} cycles before failure and is in the high stress life zone, which concludes the present work.

4.2 Future scope

As for the future scope of this work it is suggested to use Timoshenko beam elements which also includes shear deformation. And will be suitable for the short rotors. Then stress concentration due to discontinuous cross-section is also not considered, considering it would also result in higher stresses. Instead of a simple disc profiles of blades as in turbines may also be considered in the analysis. Finally an experimental setup can be done for the analyzed rotor.

4.3 References

4.3 References

[1] Nelson H.D. and McVaugh J.N., "The dynamics of rotor-bearing system using finite elements", journal of engineering for industry, vol. 98, pp. 593-600, 1976

[2] Zorzi E.S. and Nelson H.D., "Finite Element Simulation of Rotor-Bearing Systems with Internal Damping", Journal of Engineering for Power, Transactions of the ASME, vol. 99, pp. 71-76, 1977.

[3] Gujar R.A. and Bhaskar S.V., 2013, "Shaft Design under Fatigue Loading by Using Modified Goodman Method", International Journal of Engineering Research and Applications, vol. 3(4), pp.1061-1066.

[4] Goksenli A. and Eryurek I.B. 2009. , "Failure analysis of an elevator drive shaft", Journal of Engineering Failure Analysis, vol. 16, pp. 1011–1019.

[5] Mahesh L. Raotole , D. B. Sadaphale , J. R.Chaudhari, "Prediction of Fatigue Life of Crank Shaft using S-N Approach'' International Journal of Emerging Technology and Advanced Engineering, Volume 3, Issue 2, February 2013.

[6] Zorzi ES, Nelson HD. "The dynamics of rotor-bearing systems with axial torque - a finite element approach". Journal of Mechanical Design 1980; 102:158–61.

[7] Hai-jun.X, Jian.S, "Failure analysis and optimization design of a centrifuge rotor", Engineering Failure Analysis,vol 14 ,pp101–109,2014

[8] Roy H. and Dutt J.K. and Datta P.K. "The Dynamics of Multi-layered Viscoelastic Beams", Journal of Structural Engineering and Mechanics, vol. 33, pp 391-406.

[9] Muszynska A. "Forward and Backward Precession of a Vertical Anistropically Supported Rotor", Journal of Sound and Vibration 1996; vol 192(1), pp 207-222.

[10] Bauchau O.A., Craig J.I., "Euler-Bernoulli beam theory", Journal of Solid Mechanics and its application, Volume 163, 2009, pp 173-221.

[11] Lalanne M. and Ferraris G., 1998," Rotor Dynamics prediction in Engineering", John wiley and sons, Sand Sandwich Beams', Journal of composite structure 79pp411-422.

[12] Zhenxing S. and Qiang T. and Xiaoning L. and Gengkai H., "Thermally induced vibrations of flexible beams using Absolute Nodal Coordinate Formulation", Journal of Aerospace Science and Technology 29 (2013) pp 386-393.

[13] Narasimha M. and Appu K. and Ravikiran K., "Thermally induced vibration Of a simply supported beam using finite element method", International Journal of Engineering Science and Technology vol 2 (12), pp 7874-7879, 2010

[14] Taplak.H, Parlak M, "Evaluation of gas turbine rotor dynamic analysis using the finite element method" Measurement 45,pp 1089–1097,2012.

[15] Jalali M.H, Ghayour M,"Dynamic analysis of a high speed rotor-bearing system", Measurement ,vol-53,pp 1–9,2014

[16] Cook R.D., Davis S.M., Michael E.P. and Robert J.W., "Concept and Application of Finite Element Analysis", John Wiley & Sons, 2002 4th edition.

[17] Dutt J.K.,Nakra.B, "Stability characterstics of rotating systems with journal bearings on viscoelastic support" Mech. Mach. Theory, Vol. 31, No. 6, pp. 771-779, 1996

[18] Slaymaker.R.R., "Mechanical Design and Analysis'', John Willey & Sons, 1959.

[19] Bernard J.H. and Jocobson B. and Steven R.S., "Fundamentals of Machine Element'', McGraw-Hill Higher Education, 2004.

[20] Khurmi R.S. and Gupta J.K., "Machine Design'', S. Chand Publishers, 2009.

[21] Bhandari V.B., "Design of Machine Elements'', Tata McGraw-Hill Education, 2010.

[22] Norton R.L., "Machine Design-An Integrated Approach'', Pearson Education, 2003.

[23] Genta, 'Dynamics of Rotating Systems', Mechanical Engineering Series, Frederick F. Ling Series editor.

[24] Dowling.N, "Mean Stress Effects in Stress-Life and Strain-Life Fatigue", Society of Automotive Engineers, vol 51, 2004.

[25] Rao J.S., "History of rotating machinery dynamics" springer, vol-20, 2011.

[26] Savicki J.T,Bravo A.M, "Thermomechanical Behaviour of Rotor with Rubbing", International Journal of Rotating Machinery, vol 9(1),pp 41–47, 2003

4.4 Appendix

$$[M_T] = \frac{\rho \times A_r \times le}{420} \times \begin{bmatrix} 156 & 22le & 0 & 0 & 54 & -13le & 0 & 0 \\ & 4le^2 & 0 & 0 & 13le & -3le^2 & 0 & 0 \\ & & 156 & -22le^2 & 0 & 0 & 54 & 13le \\ & & & 4le^2 & 0 & 0 & -13le & -3le^2 \\ & SYMMETRIC & & & 156 & -22le & 0 & 0 \\ & & & & & 4le^2 & 0 & 0 \\ & & & & & & 156 & 22le \\ & & & & & & & 4le^2 \end{bmatrix}$$

$$[M_R] = \frac{\rho \times I_r}{30 \times le} \times \begin{bmatrix} 36 & 3le & 0 & 0 & -36 & 3le & 0 & 0 \\ & 4le^2 & 0 & 0 & -3le & -le^2 & 0 & 0 \\ & & 36 & -3le^2 & 0 & 0 & -36 & -3le \\ & & & 4le^2 & 0 & 0 & 3le & -le^2 \\ & SYMMETRIC & & & 36 & -3le & 0 & 0 \\ & & & & & 4le^2 & 0 & 0 \\ & & & & & & 36 & 3le \\ & & & & & & & 4le^2 \end{bmatrix}$$

$$q=\begin{bmatrix} y_{xy1} & \phi_{xy1} & z_{xy1} & \theta_{xy1} & y_{xz2} & \phi_{xz2} & z_{xz2} & \theta_{xz2} \end{bmatrix}$$

$$[K_B]=\frac{E\times \mathrm{I}_r}{le^3}\times\begin{bmatrix} 12 & 4le^2 & 0 & 0 & -12 & 6le & 0 & 0 \\ & 4le^2 & 0 & 0 & -6le & 2le^2 & 0 & 0 \\ & & 12 & -6le & 0 & 0 & -12 & -6le \\ & & & 4le^2 & 0 & 0 & 6le & 2le^2 \\ & SYMMETRIC & & & 12 & -6le & 0 & 0 \\ & & & & & 4le^2 & 0 & 0 \\ & & & & & & 12 & 6le \\ & & & & & & & 4le^2 \end{bmatrix}$$

$$[K_C]=\frac{E\times \mathrm{I}_r}{le^3}\times\begin{bmatrix} 0 & 0 & 12 & -6le & 0 & 0 & -12 & -6le \\ & 0 & 6le & -4le^2 & 0 & 0 & -6le & -2le^2 \\ & & 0 & 0 & 12 & -6le & 0 & 0 \\ & SKEW & & 0 & -6le & 2le^2 & 0 & 0 \\ & SYMMETRIC & & & 0 & 0 & 12 & 6le \\ & & & & & 0 & -6le & -4le^2 \\ & & & & & & 0 & 0 \\ & & & & & & & 0 \end{bmatrix}$$

$$[K_A] = \frac{P_A}{30 \times le} \times \begin{bmatrix} 36 & 3le & 0 & 0 & -36 & 3le & 0 & 0 \\ & 4le^2 & 0 & 0 & -3le & -le^2 & 0 & 0 \\ & & 36 & -3le^2 & 0 & 0 & -36 & -3le \\ & & & 4le^2 & 0 & 0 & 3le & -le^2 \\ & SYMMETRIC & & & 36 & -3le & 0 & 0 \\ & & & & & 4le^2 & 0 & 0 \\ & & & & & & 36 & 3le \\ & & & & & & & 4le^2 \end{bmatrix}$$

$$P_A = \alpha \times (\Delta T) \times E \times A_r$$

$$[K_T] = TR \times \begin{bmatrix} 0 & 0 & 0 & \frac{1}{le} & 0 & 0 & 0 & -\frac{1}{le} \\ 0 & 0 & \frac{1}{le} & \frac{1}{2} & 0 & 0 & -\frac{1}{le} & -\frac{1}{2} \\ 0 & \frac{1}{le} & 0 & 0 & 0 & -\frac{1}{le} & 0 & 0 \\ \frac{1}{le} & -\frac{1}{2} & 0 & 0 & -\frac{1}{le} & \frac{1}{2} & 0 & 0 \\ 0 & 0 & 0 & -\frac{1}{le} & 0 & 0 & 0 & \frac{1}{le} \\ 0 & 0 & -\frac{1}{le} & \frac{1}{2} & 0 & 0 & \frac{1}{le} & -\frac{1}{2} \\ 0 & -\frac{1}{le} & 0 & 0 & 0 & \frac{1}{le} & 0 & 0 \\ -\frac{1}{le} & -\frac{1}{2} & 0 & 0 & \frac{1}{le} & \frac{1}{2} & 0 & 0 \end{bmatrix}$$